Inorg. Chem. **2003**, *42*, 8504–8508

High-Field, Multifrequency EPR Study of the $[Mn(OH_2)_6]^{3+}$ Cation: Influence of π-Bonding on the Ground State Zero-Field-Splitting Parameters

Philip L. W. Tregenna-Piggott,*,† Høgni Weihe,*,‡ and Anne-Laure Barra§

Department of Chemistry, University of Bern, Freiestrasse 3, Bern 9, CH-3000, Switzerland, Department of Chemistry, University of Copenhagen, Universitetsparken 5, DK-2100 Copenhagen, Denmark, and Grenoble High Magnetic Field Laboratory, LCMI-CNRS B.P. 166, 38042 Grenoble cedex 9, France

Received July 4, 2003

High-field, multifrequency EPR data are presented for the alum $CsMn(SO_4)_2 \cdot 12D_2O$, containing the $[Mn(OD_2)_6]^{3+}$ cation. The data are interpreted using the conventional $S = 2$ spin Hamiltonian, and the following parameters determined for the data obtained below 30 K: $D = -4.491(7)$ cm^{-1}, $E = 0.248(5)$ cm^{-1}, $g_x = 1.981(5)$, $g_y = 1.993(5)$, $g_z = 1.988(5)$. Although the deviation of the MnO_6 framework from idealized D_{4h} symmetry is small, the magnitude of E/D is significant. The E parameter is related to ligand field parameters derived from the optical absorption spectrum. The rhombic anisotropy is shown to arise as a consequence of the π-anisotropic nature of the manganese(III)–water interaction.

1. Introduction

The high-field, multifrequency EPR technique has been increasingly employed to elucidate the electronic structure of non-Kramers transition metal compounds.[1,2] These studies have rendered a very precise determination of the ground-state spin-Hamiltonian parameters and have rekindled interest in ligand field theory.[2−4] Clusters and monomers containing the manganese(III) cation continue to receive particular attention, owing to their ubiquity in biology and material science,[1] the factors governing the values of the zero-field-splitting parameters being the preoccupation of a number of articles.[4−8] The rhombic zero-field-splitting parameter provides a measure of the deviation of the molecule from axial symmetry, and has been generally rationalized in terms of the relative magnitudes of the manganese−ligand bond lengths.[2,5] In this article, high-field multifrequency EPR data are presented for the cesium manganese alum, $CsMn(SO_4)_2 \cdot 12D_2O$ (CsMnSD), the molecular and electronic structure of which have been probed by elastic[9] and inelastic[10] neutron scattering experiments. This alum undergoes a cubic ($Pa\bar{3}$) to orthorhombic (*Pbca*) phase transition at ∼156 K, driven by the cooperative Jahn−Teller effect, resulting in the lowering of the site symmetry of the $[Mn(OD_2)_6]^{3+}$ cation from S_6 to C_i.[9] At 5 K, the aqua ion is tetragonally elongated, with Mn−O bond distances of 2.129(2), 1.929(1), and 1.924(1) Å, and all O−Mn−O bond angles within 1.4° of 90°. The water molecules are all rotated about the Mn−O bond vectors by the angle $\varphi \sim -19°$, depicted in Figure 1a of ref 9. Despite the deviation of the MnO_6 framework from idealized D_{4h} symmetry being only slight, the magnitude of the rhombic zero-field-splitting parameter is significant. This

* Authors to whom correspondence should be addressed. E-mail: tregenna@iac.unibe.ch (P.L.W.T.-P.); weihe@kiku.dk (H.W.).
† University of Bern.
‡ University of Copenhagen.
§ Grenoble High Magnetic Field Laboratory.

(1) Smith, G. M.; Riedi, P. C. *Electron Paramagn. Reson.* **2000**, *17*, 164.
(2) Gatteschi, D.; Sorace, L.; Sessoli, R.; Barra, A. L. *Appl. Magn. Reson.* **2001**, *21*, 299.
(3) Tregenna-Piggott, P. L. W.; Weihe, H.; Bendix, J.; Barra, A.-L.; Güdel, H.-U. *Inorg. Chem.* **1999**, *38*, 5928.
(4) Mossin, S.; Weihe, H.; Barra, A.-L. *J. Am. Chem. Soc.* **2002**, *124*, 8764.
(5) Barra, A.-L.; Gatteschi, D.; Sessoli, R.; Abbati, G. L.; Cornia, A.; Fabretti, A. C.; Uytterhoeven, M. G. *Angew. Chem., Int. Ed. Engl.* **1997**, *36*, 2329.
(6) Krzystek, J.; Telser, J.; Pardi, L. A.; Goldberg, D. P.; Hoffman, B. M.; Brunel, L.-C. *Inorg. Chem.* **1999**, *38*, 6121.
(7) Krzystek, J.; Pardi, L. A.; Brunel, L.-C.; Goldberg, D. P.; Hoffman, B. M.; Licoccia, S.; Telser, J. *Spectrochim. Acta, A* **2002**, *58A* (6), 1113.
(8) Krzystek, J.; Yeagle, G. J.; Park, J.-H.; Britt, R. D.; Meisel, M. W.; Brunel, L.-C.; Telser, J. *Inorg. Chem.* **2003**, *42*, 4610.
(9) Tregenna-Piggott, P. L. W.; Andres, H. P.; McIntyre, G. J.; Best, S. P.; Wilson, C. C.; Cowan, J. A. *Inorg. Chem.* **2003**, *42*, 1350.
(10) Basler, R.; Tregenna-Piggott, P. L. W.; Andres, H.; Dobe, C.; Güdel, H−U.; Janssen, S.; McIntyre, G. J. *J. Am. Chem. Soc.* **2001**, *123*, 3377.

10.1021/ic0347642 CCC: $25.00
Published on Web 11/15/2003

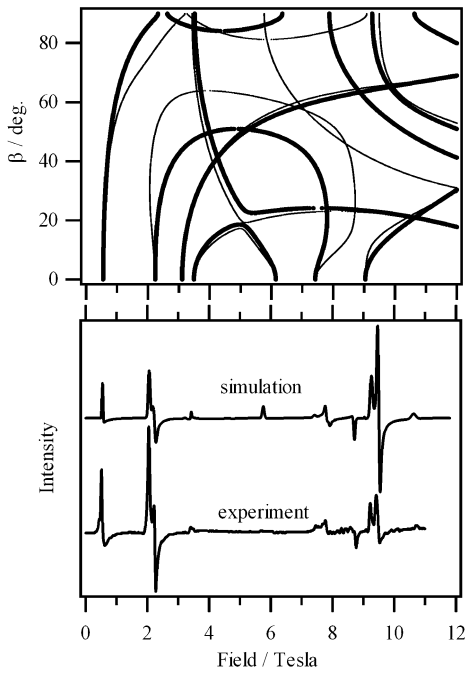

Figure 1. (a) Angular dependencies of the resonances. Thin gray and thick black lines refer to the *xz* and *yz* planes, respectively. The ordinate is the angle between the magnetic field and the molecular *z* axis. A necessary condition for a line to appear in the powder spectrum is first a nonzero transition probability for the corresponding transition as well as a vertical tangent in the corresponding angular dependence curve. (b) Experimental and simulated powder EPR spectra of $CsMn(SO_4)_2 \cdot 12D_2O$ at 60 K and 344.6985 GHz. The noise in the experimental spectrum in the range ~8−9 T is due to the coarse nature of the powder.

is shown to arise as a consequence of the π-anisotropic nature of the manganese(III)−water interaction.

2. Experimental Section

2.1. Collection of EPR Data. High-field, multifrequency EPR data were obtained for protonated and deuterated powdered samples of $CsMn(SO_4)_2 \cdot 12(H,D)_2O$, at the high magnetic field laboratory, Grenoble, France. Details of the synthesis have been provided previously.[9] The cesium manganese alum is hygroscopic and decomposes readily at room temperature. Grinding of the alum to a fine powder was, therefore, carried out in the presence of dry ice, under dry nitrogen. Powdered samples were transferred to a Teflon container, which was placed in the EPR spectrometer described previously.[11] Excitation frequencies of ca. 95, 190, 285, 345, and 380 GHz were employed in conjunction with a static field ranging from 0 to 12 T. The field was calibrated against a DPPH standard ($g = 2.0036$), measured at frequencies of ca. 95, 190, 285, 115, and 230 GHz. Spectra were recorded at temperatures ranging from 150 down to 5 K.

2.2. Collection of Electronic Spectra. A Cary 5e spectrometer was used to collect UV/vis/NIR spectra. The polished crystal was sealed in a home-built copper cell and cooled to ca. 20 K using an Air Products closed cycle refrigerator.

3. Results

3.1. EPR Data. At 150 K, no EPR lines that could be assigned to Mn(III) species were observed. Broad features could be discerned at 130 K, which sharpened and gained intensity as the sample was cooled. At 110 K, the EPR lines were sufficiently narrow to allow interpretation, using an EPR simulation program described previously.[12] Data sets were obtained at 110, 80, 40, 30, 15, and 6 K for the deuterated sample. As there appeared to be a slight variation of the resonance positions with temperature, the data sets obtained at a given temperature were analyzed independently down to 30 K, below which no notable change in the resonance positions was observed. For the protonated sample, data were obtained at 6 K only. The EPR spectra were interpreted using the spin Hamiltonian

$$\hat{H} = D\left[\hat{S}_z^2 - \frac{1}{3}S(S+1)\right] + E[\hat{S}_x^2 - \hat{S}_y^2] + g_X\mu_B B_X \hat{S}_X + g_Y\mu_B B_Y \hat{S}_Y + g_Z\mu_B B_Z \hat{S}_Z \quad (1)$$

The five spin Hamiltonian parameters were extracted from the experimental spectra by numerical diagonalization of the matrix representation of eq 1, acting in the basis of the five $S = 2$ spin functions, and minimizing the function

$$\chi^2 = \sum_{i=1}^{N}\left[\frac{B_{\mathrm{obs},i} - B_{\mathrm{calc},i}}{\sigma_i}\right]^2 \quad (2)$$

where N is the number of observations, $B_{\mathrm{obs},i}$ and $B_{\mathrm{calc},i}$ are the ith observed and calculated resonance magnetic fields, respectively, and σ_i is the measurement error associated with the ith resonance magnetic field. A total of six data sets were analyzed with N ranging from 8 to 29. No further improvement in the fits was obtained by including higher order spin-Hamiltonian terms. In Figure 1 are shown the angular dependencies of the EPR transitions calculated at a frequency of 344.6985 GHz, along with simulated and experimental spectra of the deuterated sample.

In all spectra, discrepancies in the observed and calculated intensities were found. This can be attributed to a partial alignment of the crystallites due to the strong external field, which is often observed in the high-field EPR spectra of Mn(III) complexes.[6] As well as affecting the intensities, the nonuniform distribution of crystallites also distorted the band profiles, limiting the precision with which the field position of a given resonance could be determined. This is possibly compounded by the mixing of the in-phase and out-of-phase signals. Nevertheless, the spin-Hamiltonian parameters were determined with relatively good precision. At temperatures below 30 K, values of $D = -4.491(7)$, $E = 0.248(5)$ cm^{-1}, $g_x = 1.981(5)$, $g_y = 1.993(5)$, and $g_z = 1.988(5)$ were obtained for the deuterated salt. The values of the zero-field-splitting parameters are in fair agreement with those of $D = -4.539(2)$ and $E = 0.272(9)$ cm^{-1}, derived from an earlier inelastic neutron scattering study, in the same temperature range.[10] A shift in the resonance positions occurred upon hydrogen for deuterium substitution, with the following parameters determined for the protonated salt: $D = -4.431(9)$ cm^{-1}, $E = 0.258(8)$ cm^{-1}; $g_x = 2.001(5)$, $g_y = 1.997(7)$,

(11) Muller, F.; Hopkins, A.; Coron, N.; Grynberg, M.; Brunel, L. C.; Martinez, G. *Rev. Sci. Instrum.* **1989**, *60*, 3681. Barra, A.-L.; Brunel, L. C.; Robert, J. B. *Chem. Phys. Lett.* **1990**, *165*, 107.

(12) SIM, by Høgni Weihe, Department of Chemistry, University of Copenhagen. Glerup, J.; Weihe, H. *Acta Chem. Scand.* **1991**, *45*, 444.

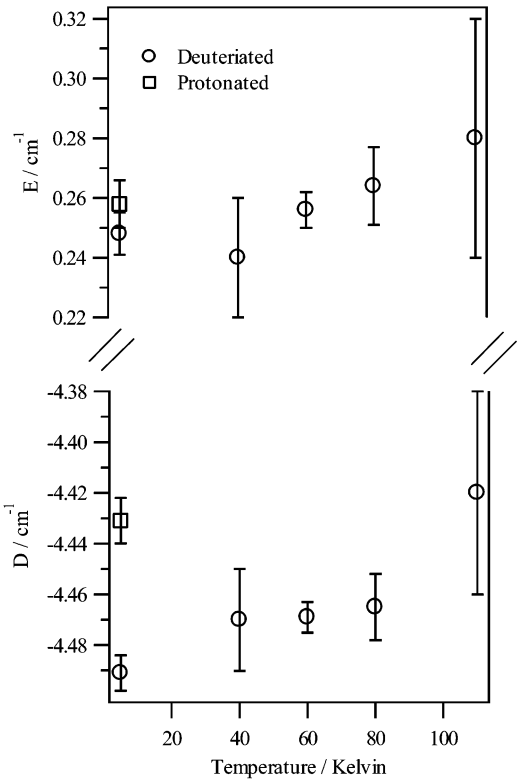

Figure 2. Dependencies of the zero-field-splitting parameters of CsMnSD on temperature and isotopic substitution.

$g_z = 1.966(12)$. Although a definite shift in the resonance positions was also observed upon change of temperature, the spin-Hamiltonian parameters could not be determined with the precision required to warrant an interpretation of the temperature dependence. The zero-field-splitting parameters determined from this study are presented in Figure 2.

3.2. Electronic Spectra. Single-crystal absorption spectra of CsMnSD were collected in the temperature range 15−200 K. The unpolarized radiation was transmitted through polished faces of the type [111] (cubic phase). At 170 K, the absorption spectrum consists of two broad bands centered at ca. 21100 and 9800 cm^{-1}. On cooling to 20 K, both features exhibit a decrease in intensity, in accordance with the vibronic origin of the intensity; the energy of the NIR band increases slightly to 10400 cm^{-1}, and the higher energy band is more structured; the spectrum is presented in Figure 3. The band maxima are similar to those recently reported for a powdered sample of CsMnSD, conducted at 80 K.[13]

In the temperature range 20−200 K, the absorption spectrum of CsMnSD is characteristic of that expected for a tetragonally distorted six-coordinate manganese(III) complex. The NIR band may be reproduced by a single Gaussian function, and is assigned as the transition between the tetragonally split components of the ^5E_g (S_6) ground term. The higher energy band is asymmetric, and is assigned as the transition from the ^5A_g (C_i) ground term to states, which in octahedral symmetry transform as components of $^5T_{2g}$. Transitions to spin-forbidden bands are also expected in this region, and our ligand field calculations suggest that these

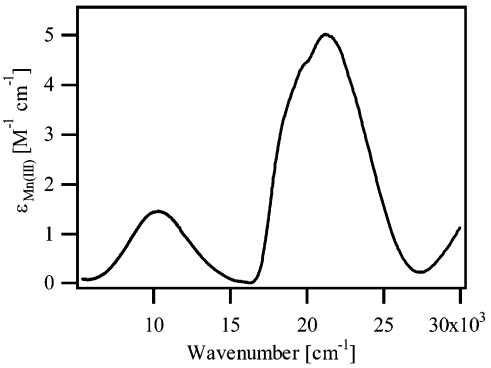

Figure 3. Single-crystal absorption spectrum of CsMnSD, recorded at 20 K.

states mix appreciably with states of the $^5T_{2g}$ (O_h) term. Hence these transitions should be broad, carry significant intensity, and will contribute to the width of the convoluted band. Attempts to fit the profile to a superposition of Gaussian functions proved unconvincing.

4. Discussion

The absorption spectrum at 170 K is characteristic of a tetragonally distorted complex, whereas the crystallographic data can be satisfactorily modeled assuming equal Mn−O bond lengths. This is because of the dynamical nature of the Jahn−Teller effect. The thermal ellipsoids at this temperature are in fact anomalous, and provide a measure of the quantity, R_{JT}: the displacement of the potential energy minimum along the $\nu_2(MnO_6)$ stretching coordinate.[9] It is this quantity which governs the energy of the intra-^5E_g transition. The energy of the NIR band and the average Mn−O bond distance increase on cooling through the phase transition. These observations are consistent with density functional theory calculations, which suggest that an increase in the average Mn−O bond length, from the 170 K value, is concomitant with a greater value of R_{JT} and hence a greater Jahn−Teller stabilization energy.[9] The room temperature absorption spectrum of the $[Mn(OH_2)_6]^{3+}$ cation in solution has also been recorded, and features centered at ca. 21000 and 14500 cm^{-1} have been identified.[14] The shift in the NIR band suggests a change in the Jahn−Teller potential energy surface, with the minima displaced farther along the $\nu_1(MnO_6)$ and $\nu_2(MnO_6)$ stretching coordinates in solution, compared to the solid state.

The angular overlap model (AOM) provides a useful framework for the interpretation of optical data of transition metal aqua ions,[15,16] and this approach is employed to model the data for CsMnSD. The observed optical absorption bands correspond to intra-^5D transitions, and depend only on the energies of the one-electron orbitals. For the ^5A_g (S_6) → ^5A_g (S_6) transition at 10400 cm^{-1}, and the ^5A_g (S_6) → $^5T_{2g}$ (O_h) at 21140 cm^{-1}, the following equations can be written down,

(13) Johnson, D. A.; Nelson, P. G. *Inorg. Chem.* **1999**, *38*, 4949.
(14) Fackler, J. P.; Chawla, I. D. *Inorg. Chem.* **1964**, *3*, 1130.
(15) Tregenna-Piggott, P. L. W.; Best, S. P.; Güdel, H. U.; Weihe, H.; Wilson, C. C. *J. Solid State Chem.* **1999,** *145*, 460.
(16) Dolder, S.; Spichiger, D.; Tregenna-Piggott, P. L. W. *Inorg. Chem.* **2003**, *42*, 1343.

relating the transition energies to the AOM bonding parameters:[17]

$$2(e_\sigma^e - e_\sigma^a) = 10400\ \text{cm}^{-1} \quad (3)$$

$$3e_\sigma^e - 4\left(\frac{e_\pi^a + 2e_\pi^e}{3}\right) = 21140\ \text{cm}^{-1} \quad (4)$$

where the superscripts a and e refer to the axial and equatorial ligands, respectively. The crystallographically inequivalent equatorial ligands are treated on the same footing, as the difference in bond lengths is barely significant (1.924(1), 1.929(1) Å). In deriving the AOM parameters appertaining to the $[Mn(OH_2)_6]^{3+}$ cation, we may be guided by spectroscopic studies on the isostructural vanadium(III) alum, from which the following parameters were proffered for the symmetric $[V(OH_2)_6]^{3+}$ cation: $e_\sigma = 6950\ \text{cm}^{-1}$; $e_\pi = 465\ \text{cm}^{-1}$, with $e_{\pi\perp} = 930\ \text{cm}^{-1}$ and $e_{\pi\parallel} = 0\ \text{cm}^{-1}$ parametrizing the π-bonding normal to—and in the plane of—the water molecule.[15] The values of the e_π parameters are expected to be more sensitive to changes in the bond lengths compared to e_σ parameters, as the molecular orbitals mediating the π-bonding interaction may be constructed from linear combinations of multipoles, that are necessarily higher in order than those mediating the σ-bonding interaction. Assuming a $1/r^6$ dependence of the e_π parameters on the bond lengths, the following parameters are obtained: $e_\pi^a = 314\ \text{cm}^{-1}$, $e_\pi^e = 572\ \text{cm}^{-1}$. From eq 1 and 2, we then obtain $e_\sigma^e = 7695\ \text{cm}^{-1}$, $e_\sigma^a = 2495\ \text{cm}^{-1}$. The large difference in the e_σ parameters incorporates the stabilization of the $3d_{z^2}$ orbital by $3d_{z^2}-4s$ mixing.[18]

The factors determining the sign and magnitude of the parameter D have been discussed extensively by several authors.[2,4−8,19] The novel aspect of the present study lies in the significant value of E, with no apparent rhombic distortion of the σ-bonding framework. For the $[Mn(OH_2)_6]^{3+}$ cation, the anisotropy is governed by the strength and nature of the π-bonding in the complex, and an analytical expression relating E to the optical spectral data may be formulated following the procedure outlined by Griffith.[20] Under the action of the spin−orbit coupling operator, the ground term interacts with several excited terms, of which $^3T_1(t_2^4)$ is the lowest in energy. To second-order in perturbation theory, the contribution from $^3T_1$ to the spin Hamiltonian parameter E is

$$E = \frac{\zeta^2}{8}\left(\frac{1}{En(^3T_1x)} - \frac{1}{En(^3T_1y)}\right) \approx \frac{\zeta^2}{8}\frac{\mu}{[En(^3T_1)]^2} \quad (5)$$

where $En(^3T_1x)$ and $En(^3T_1y)$ are the energies of the x and y components of $^3T_1$, ζ is the spin−orbit coupling parameter,

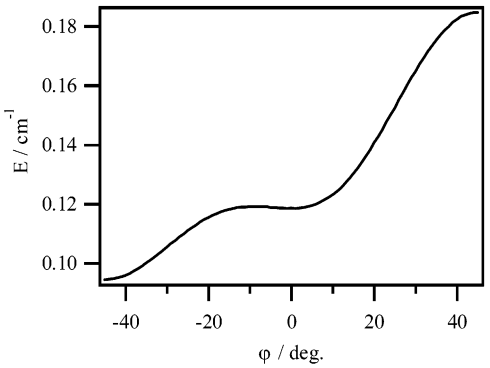

Figure 4. Variation of the zero-field-splitting parameter E, with the geometric angle, φ. The curve was calculated incorporating all terms arising from the $3d^4$ configuration with the following parameters: $e_\sigma^a = 2495\ \text{cm}^{-1}$, $e_\sigma^e = 7695\ \text{cm}^{-1}$, $e_{\pi\perp}^a = 628\ \text{cm}^{-1}$, $e_{\pi\parallel}^a = 0\ \text{cm}^{-1}$, $e_{\pi\perp}^e = 1143\ \text{cm}^{-1}$, $e_{\pi\parallel}^e = 0\ \text{cm}^{-1}$, $B = 760\ \text{cm}^{-1}$, $C = 3290\ \text{cm}^{-1}$, and $\zeta = 281\ \text{cm}^{-1}$. All O−Mn−O bond angles were set to 90°.

and $\mu = En(^3T_1y) - En(^3T_1x) = En(d_{zx}) - En(d_{yz})$. At $\varphi = 0$, μ may be expressed in terms of AOM parameters as follows:

$$\mu \approx 2[(e_{\pi\perp}^e - e_{\pi\parallel}^e) - (e_{\pi\perp}^a - e_{\pi\parallel}^a)] \quad (6)$$

Equations 5 and 6 predict a linear dependence of the parameter E upon the π-anisotropy, which is borne out by calculations performed using the program LIGFIELD,[21] incorporating all terms arising from the $3d^4$ configuration. Using the AOM parameters derived from interpreting the absorption spectrum, and setting ζ and the Racah B and C repulsion parameters arbitrarily, to 80% of the free-ion values,[22] we calculate $En(^3T_1) \approx 8000\ \text{cm}^{-1}$. Assuming the water ligand to be a pure out-of-plane π-donor, i.e., $e_{\pi\perp}^a = 628\ \text{cm}^{-1}$, $e_{\pi\parallel}^a = 0\ \text{cm}^{-1}$, $e_{\pi\perp}^e = 1143\ \text{cm}^{-1}$, $e_{\pi\parallel}^e = 0\ \text{cm}^{-1}$, E is calculated as $\sim 0.15\ \text{cm}^{-1}$ from eq 5 and 6, which compares very well to the value of $0.12\ \text{cm}^{-1}$ calculated numerically, using the full electronic basis. A complicated dependence of E upon on the angle φ is predicted, with the magnitude remaining significant for all geometries, as shown in Figure 4. The relation was calculated numerically, with all O−Mn−O bond angles set to 90°. Further calculations were carried out using the O−Mn−O angles obtained from the 5 K crystal structure, and the values of E so obtained were all found to be within 10% of those presented in Figure 4. Furthermore, setting the quantity $(e_{\pi\perp} - e_{\pi\parallel})$ to zero, E was found to decrease by an order of magnitude, demonstrating that the small rhombic perturbation of the MnO_6 framework is not responsible for the significant value of the parameter E.

For the experimental value of $\varphi = -19°$, E is calculated to be $\sim 0.12\ \text{cm}^{-1}$, which is half of that determined from the EPR measurements. Agreement could be obtained by choosing different Racah and spin−orbit coupling parameters. However, as the information available from the absorption spectrum is limited, further modeling of the data would be

(17) Schäffer, C. E. *Struct. Bonding* **1968**, 5, 68−95.
(18) Riley, M. J. *Inorg. Chim. Acta* **1998**, *268*, 55.
(19) Telser, J.; Pardi, L. A.; Krzystek, J.; Brunel, L.-C. *Inorg. Chem.* **1998**, *37*, 5769.
(20) Griffith, J. S. *The Theory of Transition-Metal Ions*; Cambridge University Press: New York, 1961; p 209.
(21) LIGFIELD ver. 0.92, by Jesper Bendix 1998, Department of Chemistry, University of Copenhagen.
(22) Bendix, J.; Brorson, M.; Schaeffer, C. E. *Inorg Chem.* **1993**, *32*, 2838−2849. Brorson, M.; Schaeffer, C. E. *Inorg. Chem.* **1988**, *27*, 2522−2530.

unwarranted. Furthermore, the foregoing analysis takes no account of dynamical Jahn−Teller coupling, which modifies the effect of certain electronic operators[23] and can give rise to a dependence of the zero-field-splitting parameters upon temperature[24] and isotopic abundance. Further experimental and theoretical work is in progress to establish the influence of the dynamical Jahn−Teller effect on the energies of the low lying electronic states.

A high-field EPR study on the isostructural $[Cr(OH_2)_6]^{2+}$ cation in frozen aqueous solution has also been reported.[19] In this medium, the $[Cr(OH_2)_6]^{2+}$ cation is reported to be "perfectly axial" with zero-field-splitting parameters $D = -2.20(5)$, $E = 0.0(1)$ cm^{-1}. Qualitatively, eq 5 and 6 account for the low E value as follows: AOM parameters for divalent transition metal aqua ions are generally between half and two-thirds of those of trivalent aqua ions. This roughly doubles $E(^3T_1)$ and halves μ. Furthermore, the ratio of the free-ion spin−orbit coupling parameters[22] is $\zeta(Cr^{2+})/\zeta(Mn^{3+}) = 229/351 = 0.65$. Collecting these factors we obtain $E[Cr(OH_2)_6]^{2+}/E[Mn(OH_2)_6]^{3+} \approx 0.1$, in agreement with experiment. Finally, for the $[Mn(OH_2)_6]^{3+}$ cation in $CsMn(SO_4)_2 \cdot 12D_2O$, the mode of water coordination is trigonal planar, which maximizes ($e_{\pi\perp} - e_{\pi\parallel}$). The π-anisotropy is known to be reduced significantly for trigonal pyramidal coordination.[25,26]

5. Conclusion

High-field, multifrequency EPR data have been presented, providing a precise characterization of the ground-state electronic structure, as a function of temperature. The magnitude of the orthorhombic zero-field-splitting parameter, E, is significant, despite the MnO_6 framework being close to idealized D_{4h} symmetry. The value of E in this system is governed largely by the energy of the higher-lying $^3T_{1g}$ (O_h) term, the π-anisotropic nature of the manganese(III)−water interaction, and the disposition of the water molecules. This study demonstrates that although the nature of the metal−ligand π-interaction has a negligible effect on the Jahn−Teller interaction in manganese(III) complexes, it plays a significant role in determining the resulting magnetic anisotropy.

Acknowledgment. This work was funded by the Swiss national science foundation. The EPR laboratory of GHMFL is part of the EC SENTINEL network (Programme No. HPRI-CT-2000-40022).

IC0347642

(23) Ham, F. S. *J. Phys. Colloq.* **1971**, *32*, 952.
(24) Dobe, C.; Tregenna-Piggott, P. L. W.; Mossin, S.; Weihe, H.; Janssen, S. *Chem. Phys. Lett.* **2002**, *362*, 387−396.
(25) Spichiger, D.; Carver, G.; Dobe, C.; Bendix, J.; Tregenna-Piggott, P. L. W.; Meier, R.; Zahn, G. *Chem. Phys. Lett.* **2001**, *337*, 391.
(26) Riesen, H.; Dubicki, L. *Inorg. Chem.* **2000**, *39*, 2206.